CHEMISTRY
A European Journal

A Journal of
ChemPubSoc Europe

Accepted Article

Title: A fluorescence lifetime based binding assay for class IIa histone deacetylases

Authors: Christian Meyners, Monique Mertens, Pablo Wessig, and Franz-Josef Meyer-Almes

To be cited as: *Chem. Eur. J.* 10.1002/chem.201605140

Link to VoR: http://dx.doi.org/10.1002/chem.201605140

Supported by
ACES

WILEY-VCH

10.1002/chem.201605140

WILEY-VCH

A fluorescence lifetime based binding assay for class IIa histone deacetylases

Christian Meyners[a], Monique Mertens[b], Pablo Wessig*[b] and Franz-Josef Meyer-Almes*[a]

Abstract: Class IIa HDACs show extremely low enzymatic activity and no commonly accepted endogenous substrate is known today. Increasing evidence suggests that these enzymes exert their effect rather through molecular recognition of acetylated proteins and recruiting other proteins like HDAC3 to the desired target location. Accordingly, class IIa HDACs like bromodomains have been suggested to act as “Readers” of acetyl marks, whereas enzymatically active HDACs from class I or IIb are called “Erasers” to highlight their capability to remove acetyl groups from acetylated histones or other proteins. Small molecule ligands of class IIa histone deacetylases (HDACs) gained tremendous attention during the last decade and were suggested as pharmaceutical target in several indication areas such as cancer, Huntington’s disease or muscular atrophy. Up to now only enzyme activity assays with artificial chemically activated trifluoroacetylated substrates are in use for the identification and characterization of new active compounds against class IIa HDACs. Here, we describe the first binding assay for this class of HDAC enzymes with simple mix-and-measure procedure and extraordinary robust fluorescence lifetime readout based on [1,3]dioxolo[4,5-*f*]benzodioxole-based ligand probes. The assay principle is generic and can also be transferred to class I HDAC8.

Introduction

Members of the histone deacetylase (HDAC) family have emerged as promising protein target for the treatment of different diseases like cancer, neurodegenerative diseases and parasitic infections.[1-3] The 18 human members of the HDAC family are divided into four classes: Class I consists of HDAC1, 2, 3 and 8, class II HDACs are subdivided into class IIa (HDAC4, 5, 7 and 9) and IIb (HDAC6 and 10), HDAC11 is the only member of class IV and the sirtuins which are class III HDACs are not zinc dependent but require NAD^+ for their catalytic activity.[4] Class I HDACs are mostly recognised for their ability to control the expression of important genes via the deacetylation of lysine residues of histone proteins.[5] They have therefore emerged to be the number one target of all HDAC proteins. Currently, there are four HDAC inhibitors approved by the FDA for the treatment of cancer and several more are tested in clinical trials.[6] Most of these compounds are pan inhibitors, which target mainly class I and class IIb HDACs and cause severe side effects like fatigue, nausea and thrombocytopenia.[7,8] An approach to overcome these unwanted side effects is the development of more specific inhibitors. Class IIa HDACs are different from other HDAC isoforms since they show very week catalytic activity against conventional acetylated substrates and have a large N-terminal domain through which they interact with several transcription factors.[9] Furthermore, they are able to recruit class I HDACs via protein-protein interactions resulting in large corepressor complexes like NcoR and CoREST.[10] There has been an extensive scientific dispute whether class IIa HDACs possess endogeneous catalytic activity In fact, the catalytic deacetylation activity is about 1000-fold weaker than in class I HDACs and there is no commonly accepted specific substrate identified for class IIa enzymes today.[9,11,12] However, if class IIa HDACs are immunoprecipitated, a lysine deacetylase activity can be measured which is most likely due to co-purified class I HDACs.[13-15] The vanishing activity of class IIa HDACs can be dramatically increased, by a H967Y mutation, whereas a mutation of the corresponding Y into H in class I HDACs leads to inactivation confirming that class IIa HDACs are very inefficient deacetylases due to this difference in a pivotal amino acid position.[9] Furthermore, transcriptional repression of MEF2 by HDAC4 was shown to be mediated only by protein-protein interaction and not to depend on deacetylase activity.[9,16] Accordingly, class IIa HDACs have also been suggested as epigenetic readers of acetyl marks with dissociation constants within the range of binding affinities reported for bromodomains (K_d = 10-100µM).[17-19] These findings have culminated in the currently broadly accepted view of a mostly non-catalytic role of class IIa HDACs.[11,17,20-22] Although their function is as yet little understood huge effort has been directed towards the development of specific HDAC class IIa inhibitors.[20,23] The therapeutic indication area for HDAC class IIa inhibitors range from cancer to neurodegenerative diseases like Chorea Huntington.[14,22,24] The ongoing efforts in the development of HDAC inhibitors and the large pharmacological interest clearly indicate an urgent need for devoted assays suitable for high throughput screening (HTS) campaigns. Most commercially available assay systems for the evaluation of HDAC inhibitors rely on the deacetylation of a substrate and subsequent enzymatic conversion into a quantifiable fluorophore.[25-27] As class IIa HDACs are believed to act mainly as readers that recognise acetylated lysines, chemically activated substrates were developed exploiting a trifluoroacetyled lysine.[28] Direct HDAC binding assays rely on the displacement of usually hydroxamic acid based probes.[29-32] Recently, such an assay was published for HDAC like prokaryotic enzymes. The authors used the environment sensitivity of [1,3]dioxolo[4,5-*f*]benzodioxole (DBD) dyes to monitor the binding of a hydroxamic acid DBD conjugate via a large change of its fluorescence lifetime upon binding. Thus a stable signal was produced, which was insensitive to autofluorescence in the UV region. The presented assay was further exploited to determine

[a] C.Meyners, Prof. Dr. F.-J. Meyer-Almes
Fachbereich Chemie- und Biotechnologie
Hochschule Darmstadt
Haardtring 100, 64295 Darmstadt (Germany)
E-mail: franz-josef.meyer-almes@h-da.de
[b] M. Mertens, Prof. Dr. P. Wessig
Institut für Chemie
Universität Potsdam
Karl-Liebknecht-Str. 24-25, 14476 Potsdam (Germany)
E-mail: wessig@uni-potsdam.de

Supporting information for this article is given via a link at the end of the document.

the affinity of a set of HDAC inhibitors using a competitive binding assay.[33] Unfortunately, these probes are not applicable to class IIa HDACs as hydroxamic acids are known to be mostly weak inhibitors of these enzymes.[34,35] In fact, until today there is a lack of direct binding assays for HDAC class IIa enzymes although molecular recognition of acetylated lysine residues is supposed to be their primary mode of action. In this study, a binding assay is developed to fill this gap and meet the urgent need for a binding assay applicable to class IIa HDACs.

Results and Discussion

The assay development was inspired by a binding assay for class I and IIb HDACs using a ligand probe containing a hydroxamate group. In this study a series of DBD probes with a trifluoromethylketone (TFMK) pharmacophoric group instead of a hydroxamic acid were synthesised, since compounds containing a TFMK group have been described as reasonable ligands for class IIa HDACs.[35,36]

For the synthesis of the DBD ligands a convergent route, shown in scheme 1, was chosen. Starting with the synthesis of DBD amines **6** and **7** by coupling of the known acyl and ester DBD acids **1** and **2** to *N*-boc protected diethylamine **3**, the intermediates **4**,**5** were subsequently deprotected catalysed by trifluoroacetic acid (TFA).[37] For the TFMK building blocks the synthesis of **12a**,**b** starts with commercially available glutaric acid diethyl ester (**10a**) and adipic acid monomethyl ester (**10b**). The synthesis of **12c** starts with compound **10c** which was synthesised by dehydration of pimelic acid **8** with acetic anhydride as dehydration agent according to the known procedure of Cisneros *et al.* and solvolysis of the resulting anhydride **9** with methanol.[38] Although the diethyl ester **10a** was transferred to the corresponding TFMK **12a** according to the procedure of Okano *et al.*, this procedure has not worked for the preparation of the TFMKs **12b,c**.[39] Therefore another route was used, which starts with conversion of the carboxylic moieties of **10b,c** to the TFMKs **11b,c** with conditions described by Biovin *et al.*.[40] Then, the monomethyl ester moieties were saponified with lithium hydroxide to give the TFMKs **12b,c** similar to the procedure of Frey *et al.*.[36] Finally the DBD amines **6**,**7** are coupled to the TFMKs **12a-c** under standard peptide coupling conditions.

Especially for compounds **13**,**14a** a mixture of two tautomers was observed, where the cyclic forms **13**,**14a'** exist predominantly to the linear in $CDCl_3$, shown in scheme 2. Dissolving the samples in MeOH leads to a shift of equilibrium to the linear forms **13**,**14a**. This could be shown by ^{19}F-NMR, where the samples were concentrated from methanol and subsequently spectra in $CDCl_3$ were recorded (Fig. S1 and S2). Specifically, for **13a** a ratio of 1:1 between **13a** and **13a'** could be observed. Recording a second spectrum after a few hours showed a ratio of 10:1 with **13a'** as the predominant form. A similar behaviour was monitored for compound **14a**. Thus we assume a dynamic equilibrium between the different tautomers depending on the solvent.

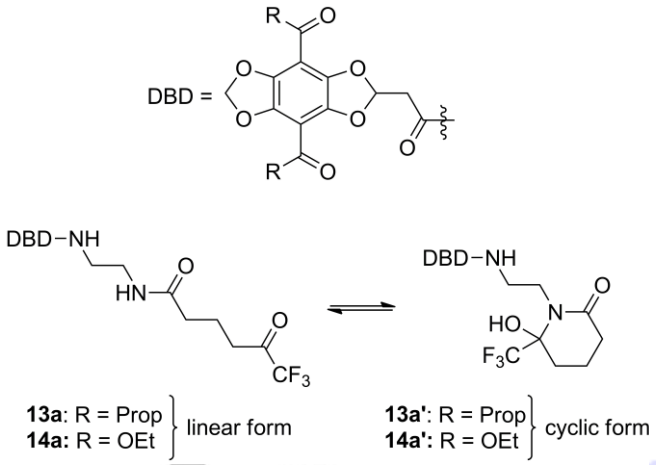

Scheme 2. Dynamic equilibrium between to tautomers of compound **13,14a**.

10.1002/chem.201605140

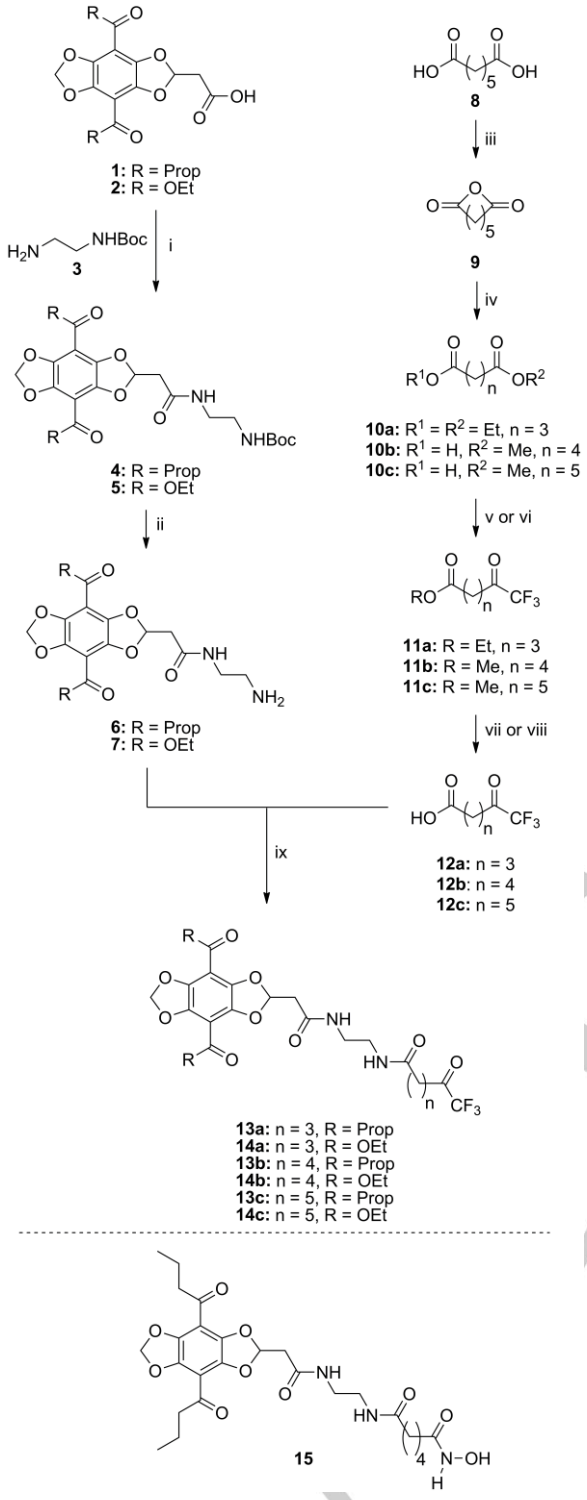

Scheme 1. Synthesis of DBD dyes **13a-c** and **14a-c**. Reagents and conditions: i) 1. $(COCl)_2$, DCM, DMF, 30 min 0°C, then rt; 2.) DIEA, DCM, **3** (**4:** 87 %, **5:** 90 %); ii) TFA, DCM (**6:** 94 %, **7:** 98 %); iii) Ac_2O, reflux; iv) MeOH, reflux (**10c:** over 2 steps 51 %); v) NaOEt, CF_3COOEt, reflux; vi) 1.) $(COCl)_2$, DCM, DMF, 30 min 0°C, then rt; 2.) TFAA, Pyridine, 0°C; vii) 30 % H_2SO_4, reflux (**12a:** over 2 steps 17 %); viii) LiOH, THF, H_2O (over 2 steps: **12b:** 41 %, **12c:** 35 %); ix) TBTU, DIEA, DMF (**13a:** 89 %, **13b:** 71 %, **13c:** 90 %, **14a:** 84 %, **14b:** 89 %, **14c:** 98 %).

The obtained ligands were first analysed for their potential to inhibit human HDAC1-8. As expected the hydroxamic acid DBD probe **15** was inactive towards class IIa HDACs and active towards the other HDAC isoforms (Table. 1). In contrast, **13b** with TFMK moiety showed inhibitory activity against class IIa HDACs in the micromolar range and preference for HDAC3 and 8. While the reduction of the spacer to 3 CH_2 units of **13a** resulted in a mostly inactive compound, the increment by one spacer unit from 4 to 5 CH_2 units of **13c** resulted in an increase of the inhibitory activity. This effect was stronger pronounced on class IIa HDACs with factors between 14 and 220, compared to factors between 2 and 5 for the other HDACs. Similar observations were made for the ester variants **14a-c** of the DBD probes, which showed in general IC_{50}-values similar to the acyl DBD probes **13a-c**. Only the inhibition of HDAC8 by **14a** was about 15 times stronger than for its acyl counterpart.

10.1002/chem.201605140

Table 1. Inhibition of HDACs by DBD probes. IC_{50}-values (µM) were determined using a fluorogenic enzyme activity assay as described in the experimental section.

Probe	HDAC1	HDAC2	HDAC3	HDAC4	HDAC5	HDAC6	HDAC7	HDAC8
13a	>50	>50	>50	10±1	4.0±1.0	>50	1.9±0.2	4.8±0.3
13b	1.6±0.1	7.6±0.4	0.11±0.01	2.2±0.3	1.4±0.2	3.8±0.2	1.6±0.1	0.091±0.008
13c	0.82±0.03	3.2±0.1	0.042±0.003	0.010±0.002	0.10±0.01	0.79±0.1	0.036±0.006	0.021±0.001
14a	>50	>50	>50	14±1	5.3±0.5	>50	3.6±0.2	0.31±0.02
14b	2.5±0.1	21±1	0.18±0.01	3.9±0.2	2.4±0.1	2.9±0.5	2.5±0.1	0.14±0.01
14c	1.0±0.1	4.3±0.4	0.075±0.002	0.032±0.002	0.21±0.03	1.0±0.1	0.030±0.009	0.058±0.003
15	0.53±0.02	1.0±0.03	2.5±0.5	>50	>50	5.2±0.9	>50	3.2±0.3

Next, the change of FLT upon binding of the DBD ligands to HDAC isoforms 4, 5, 7 and 8 was measured in titration experiments. The unbound acyl probes exhibited a FLT in the range of 1.6 ns. Upon addition of the respective HDAC isoform the FLT of the DBD probes **13b** and **13c** increased in a concentration dependent manner, while binding of **13a** was not detectable in the investigated concentration range (Fig. 1 and Table 2). The largest change in FLT was determined for the binding of **13b** to HDAC4 with a difference of 6.1 ns. In general the shorter probe **13b** exhibited with at least 1.9 ns a larger change in FLT than the prolonged probe **13c**, which showed differences between 0.89 and 1.9 ns. The concentration dependency of the change in the FLT of the DBD probes was further exploited to determine the K_d-values for the binding. The determined K_d-values were comparable to the determined IC_{50}-values and were found to be between 1.2 µM and 0.01 µM. The strong increase in affinity upon increment of the spacer by one CH_2 unit towards class IIa HDACs was confirmed by the determined K_d-values. For binding to HDAC8 both probes behaved quite equal and bound with a comparable affinity and exhibited a similar change in their FLT.

The ester variants exhibited a long FLT of 25 ns in their unbound state, which theoretically decreases upon binding. Unfortunately, this was only observable for the binding of **14a** to HDAC8. Here the FLT decreased by 13 ns and it was possible to determine a K_d-value of 0.69 µM (Table 2 and Fig. S3). The other ester variants showed no difference in their FLT neither for the binding to HDAC8 nor for the binding to class IIa HDACs.

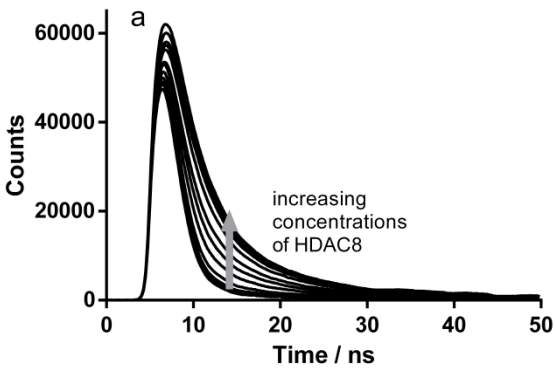

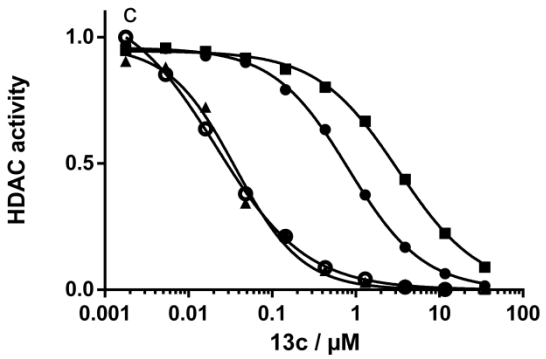

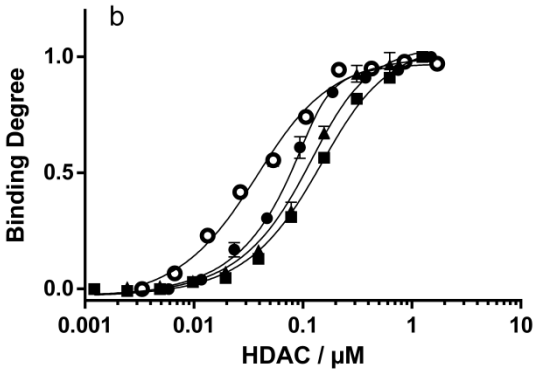

Figure 1. Binding of DBD probe **13c** to HDACs. Fluorescence decay curves of 0.025 nM **13c** in the presence of increasing HDAC8 concentrations (a). The binding of the DBD probe resulted in a concentration dependent increase in the FLT of the probe, which was exploited to determine the binding degree as described in the experimental section. The binding degree of **13c** is plotted against the concentration of HDAC4 (dots), HDAC5 (squares), HDAC7 (triangles) or HDAC8 (circles)(b). The continuous line represents the calculated fit curve to equation 3. The determined binding constants are summarised in Table 2. Inhibition of enzymatic HDAC activity by the DBD probe **13c** (c). HDAC activity of HDAC1 (dots), HDAC2 (squares), HDAC7 (triangles) and HDAC8 (circles) was determined as described in the experimental section. The continuous line represents the calculated fit curve to equation 1, which yields the IC_{50}-values summarized in Table 1.

Table 2. Changes in FLT and binding constants, K_d, of the binding of DBD probes to HDAC4, 5, 7 and 8.

Probe	HDAC4		HDAC5		HDAC7		HDAC8	
	K_d / µM	ΔFLT / ns	K_d / µM	ΔFLT / ns	K_d / µM	ΔFLT / ns	K_d / µM	ΔFLT / ns
13a	>10	-	>10	-	>10	-	>10	-
13b	1.2±0.2	6.1±0.2	0.40±0.03	1.92±0.05	0.38±0.04	3.9±0.1	0.051±0.006	2.43±0.06
13c	0.010±0.003	0.89±0.02	0.078±0.008	1.28±0.03	0.046±0.008	1.23±0.03	0.024±0.003	1.87±0.05
14a	-	-	-	-	-	-	0.69±0.06	−13.2±0.3

In order to determine the specificity of the binding and to simulate the performance of the assay under screening conditions a number of known HDAC inhibitors were used in typical screening concentrations and incubated with HDAC4 or 8 and 50 nM of the DBD probe **13b**. After an incubation of one hour the fluorescence decay was measured and the FLT was determined. Compared to the FLT of the HDAC probe complex a decrease of the FLT was observable for all HDAC inhibitors (Fig. 2). Thereby, the weak HDAC4 and HDAC8 inhibitors e.g. SAHA and TSA showed a smaller decrease of the FLT than the stronger competitors SATFMK and PDF306. Furthermore, the specific reference inhibitors PCI-34051 and TMP269 were both only active on their respective target HDAC isoform.

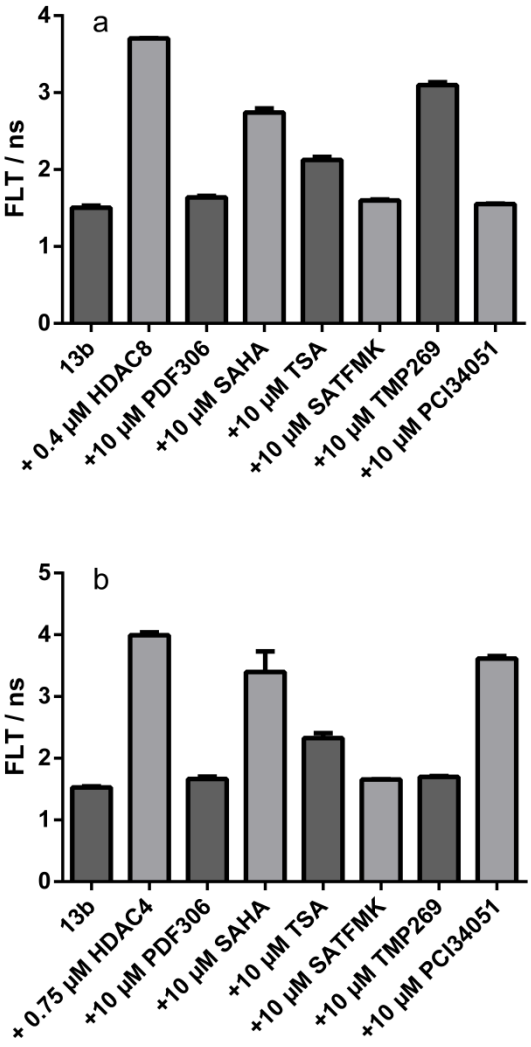

Figure 2. Displacement of the DBD **13b** by competitive HDAC inhibitors. The FLT of 0.125 µM of the DBD probe **13b** was measured alone, in presence of 0.4 µM HDAC8 (a) or 0.75 µM HDAC4 (b) and with addition of 10 µM of the indicated inhibitor.

For the strong competitors the concentration dependency of the displacement of the probe was exploited to determine the respective K_I-values. The resulting curves for binding to HDAC4 and the probe **13b** were quite steep and produced equal K_I-values around 0.08 µM for all three inhibitors (Fig. S4). This and the high error in the determined K_I-values indicated that these values could not be determined reliably, which originates presumably from the high difference in affinity between the probe and the inhibitors. To overcome these limitations the more affine binding probe **13c** was used. The resulting curves allowed a more exact determination of the K_I-values, which were in good agreement with K_d-values determined by ITC and IC_{50}-values from an enzyme activity assay (Fig. 3, Fig. S5 and Table 2). For HDAC8 the binding of the probe **13b** was more affine, which allowed a reliable determination of the K_I-values of the tested compounds.

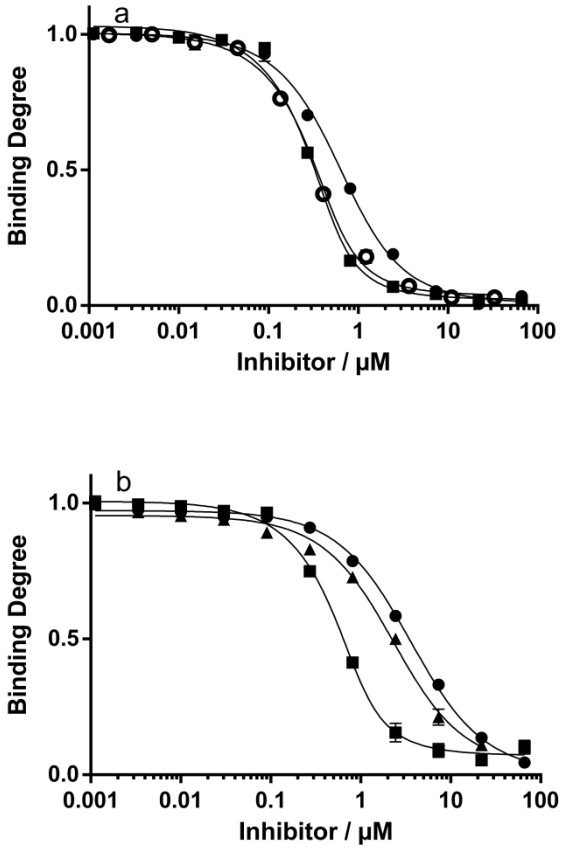

Figure 3. Determination of binding constants of the binding of unlabeled HDAC inhibitors to HDAC8 (a) and HDAC4 (b). A serial dilution of the unlabeled HDAC inhibitors PDF306 (dots), SATFMK (squares), TMP269 (triangles) or PCI34051 (circles) was incubated with either 0.45 µM HDAC8 and 0.125 µM of the DBD probe **13b** or 0.8 µM HDAC4 and 0.125 µM of the DBD probe **13c**. After equilibration the FLT of the probes was measured and translated into binding degree as described in the experimental section. The continuous line represents the calculated fit to equation 4, which yields the binding constants summarised in Table 3.

Table 3. Comparison of inhibitor binding constants, K_I determined by the fluorescence life time binding assay with K_d-values determined by ITC and IC_{50}-values of inhibitors of HDAC4 and HDAC8.

	HDAC4			HDAC8		
Compd	K_I / µM	K_d / µM	IC_{50} / µM	K_I / µM	K_d / µM	IC_{50} / µM
SATFMK	0.012 ±0.003	0.047 ±0.01	0.10 ±0.01	0.023 ±0.005	0.08 ±0.01	0.035 ±0.002

PDF306	0.23 ±0.02	0.22 ±0.04	0.40 ±0.02	0.12 ±0.01	0.058 ±0.01	0.18 ±0.06
TMP269	0.14 ±0.01	-	0.26 ±0.03	-	-	-
PCI34051	-	-	-	0.028 ±0.006	-	0.024 ±0.002

Conclusions

The presented assay is the first reported direct binding assay for class IIa HDACs. The assay relies on DBD probes which show a large change in FLT up to 6.1 ns upon binding to the enzymes. The general procedure is extremely simple (mix and measure), without any additional incubation step for the reactions of target and/or detection enzymes and exploits the proven robust FLT readout resulting in a high performance assay suitable for HTS applications. The assay is capable to identify strong as well as weak ligands under typical screening conditions and the binding constants of strong binders can be determined reliably showing good correlation with IC_{50}-values determined by enzyme activity assays. The inhibitory activity of the DBD probes against other HDAC isoforms also suggest that they may be used as generic tools in binding assays for class I and IIb HDACs.

Experimental Section

All reagents and solvents were purchased from commercial suppliers and used with further purification only if necessary. SAHA was bought from Cayman chemicals, TSA and PCI-34051 were bought from Selleckchem. HDAC isoforms 1, 2, 3 and 6 were ordered from BPS Bioscience. The compounds SATFMK, PDF306 and **15** were made as described elsewhere.[33,41,42] SUMO protease 1 (Ulp 1) was made as described by Malakhov *et al.*.[43] Reactions were performed under an inert atmosphere (nitrogen or argon) whenever anhydrous solvents were used and were monitored by thin layer chromatography (TLC) using aluminium sheets coated with silica gel (SiO_2-60, F254). Flash chromatography was carried out on silica gel 60 (40-63 µm). NMR spectra were recorded on a Bruker Avance 300. Chemical shifts are reported as δ in parts per million (ppm) relative to the solvent signal (^{1}H-NMR: $CDCl_3$ 7.26 ppm, MeOD-d_4 3.31 ppm, ^{13}C-NMR: $CDCl_3$ 77.0 ppm, MeOD-d_4 49.15 ppm). For ^{19}F-NMR trifluoroacetic acid (TFA) (-76.55 ppm) was used as external standard. Assignments of NMR spectra are based on correlation spectroscopy (COSY, HSQC). High resolution mass spectra (HRMS) were measured on a quadrupole time-of-flight (TOF) mass spectrometer. Melting points are uncorrected and were determined in an Elektrothermal 9100 melting point instrument. IR spectra were recorded on a Perkin Elmer FTIR spectrometer Spectrum 2.

Synthesis of DBD-Probes

Notice:

Some compounds with a DBD backbone show in the ^{1}H-NMR spectra signals of an AB-system caused by the methylene group belonging to the DBD. This will be marked as “AB” and the given value in Hz is the distance between the inner signals of such a spin system. The outer signals of higher order are usually too small to be able to perform analysis.

***tert*-Butyl (2-(2-(4,8-dibutyrylbenzo[1,2-d:4,5-d']bis([1,3]dioxole)-2-yl)acetamido)ethyl)-carbamate (4):** To a cooled solution (0°C) of the carboxylic acid **1** (102.4 mg, 281.05 µmol) in anhydrous DCM (25 mL) was added oxalyl chloride (0.2 mL, 2.33 mmol, 8.3 eq.) and one drop of anhydrous DMF. After 4 h the solution was concentrated under reduced pressure. The resulting solid was dissolved in anhydrous DCM (20 mL) and slowly dropped to a solution of DIEA (100 µL, 574.09 µmol, 2.0 eq.) and *tert*-butyl (2-aminoethyl)carbamate **3** (50 µL, 324.56 µmol, 1.1 eq.) in anhydrous DCM (20 mL). The solution was stirred over night for 18 h and then put into a saturated aqueous solution of $NaHCO_3$ (50 mL). The aqueous phase was extracted with DCM (4x50 mL), washed with aqueous HCl (0.1 N, 1x50 mL) and with saturated aqueous NaCl (1x50 mL). The combined organic phases were dried ($MgSO_4$), filtered and concentrated under reduced pressure. The residue was purified by silica gel chromatography (DCM/MeOH 99:1→ 92:8) to afford **4** as an orange solid (124.4 mg, 87 %). R_f = 0.50 (DCM/MeOH 25:1); m. p.: 164-165°C; ^{1}H-NMR (300 MHz, $CDCl_3$, 27°C): δ = 6.75 (bs, 1H, NH); 6.62 (t, ^3J = 5.2 Hz, 1H, CH); 6.09 (s, 2H, CH_2); 5.30 (bs, 1H, NH); 3.46-3.34 (m, 2H, CH_2); 3.33-3.19 (m, 2H, CH_2); 2.89 (d, ^3J = 5.0 Hz, 2H, CH_2); 2.87 (t, ^3J = 7.2 Hz, 4H, CH_2); 1.76-1.62 (m, 4H, CH_2); 1.41 (s, 9H, CH_3); 0.96 ppm (t, ^3J = 7.4 Hz, 6H, CH_3); ^{13}C-NMR (75 MHz, $CDCl_3$, 27°C): δ = 196.4 (2C, C=O); 166.8 (1C, C=O); 156.8 (1C, C=O); 141.1 (2C, $C_{quart.}$); 140.4 (2C, $C_{quart.}$); 110.5 (1C, CH); 110.0 (2C, $C_{quart.}$); 102.6 (1C, CH_2); 79.6 (1C, $C_{quart.}$); 45.6 (2C, CH_2); 42.0 (1C, CH_2); 40.8 (1C, CH_2); 40.3 (1C, CH_2); 28.3 (3C, CH_3); 17.1 (2C, CH_2); 13.7 ppm (2C, CH_3); IR (ATR): $\bar{\nu}$ = 3293, 2966, 1682, 1654, 1436, 1279, 1236, 1175, 1087, 1036 cm^{-1}; HRMS: (EI) *m/z* = 506.2272 [M^+], calc.: 506.2264.

Diethyl 2-(2-((2-((*tert* butoxycarbonyl)amino)- ethyl)amino)-2-oxoethyl)benzo[1,2-d:4,5-d']bis- ([1,3]dioxole)-4,8-dicarboxylate (5): Compound **5** was synthesised from the carboxylic acid **2** (98.7 mg, 267.99 µmol) by following the procedure described above for compound **4.** The desired product was obtained as yellow solid (123.3 mg, 90 %). R_f = 0.34 (DCM/MeOH 25:1); m. p.: 165-167°C; ^{1}H-NMR (300 MHz, $CDCl_3$, 27°C): δ = 6.61 (t, ^3J = 5.3 Hz, 1H, CH); 6.10 (AB, J = 0.46 Hz, 2H, CH_2); 5.26 (bs, 1H, NH); 4.38 (q, ^3J = 7.1 Hz, 4H, CH_2); 3.44-3.33 (m, 2H, CH_2); 3.33-3.20 (2H, CH_2); 2.90 (d, ^3J = 5.3 Hz, 2H, CH_2); 1.41 (s, 9H, CH_3); 1.36 ppm (t, ^3J = 7.1 Hz, 6H, CH_3); ^{13}C-NMR (75 MHz, $CDCl_3$, 27°C): δ = 166.8 (1C, C=O); 161.8 (2C, C=O); 156.6 (1C, C=O); 141.9 (2C, $C_{quart.}$); 141.2 (2C, $C_{quart.}$); 110.7 (1C, CH); 103.2 (2C, $C_{quart.}$); 102.9 (1C, CH_2); 79.5 (1C, $C_{quart.}$); 61.7 (2C, CH_2); 42.1 (1C, CH_2); 40.5 (1C, CH_2); 40.3 (1C, CH_2); 28.3 (3C, CH_3); 14.2 ppm (2C, CH_3); IR (ATR): $\bar{\nu}$ = 3275, 2977 1710, 1656, 1450, 1294, 1261, 1155, 1080 cm^{-1}; HRMS: (EI) *m/z* = 510.1840 [M^+], calc.: 510.1850.

2-(2-(4,8-Dibutyrylbenzo[1,2-d:4,5-d']bis([1,3]dioxole)-2-yl)acetamido)ethan-1-aminium 2,2,2-trifluoroacetate (6): To a solution of DCM/TFA (3:1, 12 mL) was added compound **4** (96.0 mg, 189.52 µmol). After 30 min all volatile compounds are removed and the residue was suspended in toluene. The solvent was removed under reduced pressure and this procedure was repeated once again. Then the crude product was dissolved in hot MeOH, cooled to RT and precipitated with PE. Filtration and drying under reduced pressure yield to the title compound **6** as an orange solid (92.4 mg, 94 %). m. p.: 149-151°C; ^{1}H-NMR (300 MHz, [D_4]MeOH, 25°C): δ = 6.67 (t, ^3J = 5.3 Hz, 1H, CH), 6.14 (AB, J = 1.2 Hz, 2H, CH_2), 3.54 (t, ^3J = 5.9 Hz, 2H, CH_2), 3.14 (t, ^3J = 5.9 Hz, 2H, CH_2), 3.00 (d, ^3J = 5.3 Hz, 2H, CH_2), 2.96 (t, ^3J = 7.2 Hz,

4H, CH_2), 1.82-1.60 (m, 4H, CH_2), 1.00 ppm (t, ^3J = 7.4 Hz, 6H, CH_3); ^{13}C-NMR (75 MHz, [D_4]MeOH, 25°C): δ = 199.0 (2C, C=O), 171.6 (1C, C=O), 143.4 (2C, $C_{quart.}$), 142.6 (2C, $C_{quart.}$), 113.1 (1C, CH), 112.0 (2C, $C_{quart.}$), 104.9 (1C, CH_2), 47.4 (2C, CH_2), 43.0 (1C, CH_2), 41.7 (1C, CH_2), 39.0 (1C, CH_2), 19.0 (2C, CH_2), 14.9 ppm (2C, CH_3); IR (ATR): $\tilde{\nu}$ = 3275, 3099, 2964, 1660, 1567, 1439, 1282, 1187, 1119, 1039, 837, 723 cm^{-1}; HRMS: (ESI) *m/z* = 407.1811 [MH^+], calc.: 407.1818.

2-(2-(4,8-Bis(ethoxycarbonyl)benzo[1,2-d:4,5-d']bis([1,3]dioxole)-2-yl)acetamido)ethan-1-aminium 2,2,2-trifluoroacetate (7): Compound **7** was synthesised from **5** (60.2 mg, 117.92 µmol) by following the procedure described above for compound **6.** The desired product was obtained as yellow solid (60.8 mg, 98 %). m. p.: decomp. at 176°C; ^{1}H-NMR (300 MHz, [D_6]DMSO, 25°C): δ = 8.33 (t, ^3J = 5.4 Hz, 1H, NH); 7.87 (bs, 3H, NH); 6.62 (t, ^3J = 5.2 Hz, 1H, CH); 6.12 (s, 2H, CH_2); 4.28 (q, ^3J = 7.1 Hz, 4H, CH_2); 3.43-3.28 (2H, CH_2); 2.88 (d, 2H, ^3J = 5.3, CH_2); 2.88-2.83 (2H, CH_2); 1.26 ppm (t, ^3J = 7.1 Hz, 6H, CH_3); ^{13}C-NMR (75 MHz, [D_6]DMSO, 25°C): δ = 168.1 (1C, C=O); 161.8 (2C, C=O); 141.9 (2C, $C_{quart.}$); 141.8 (2C, $C_{quart.}$); 112.1 (1C, CH); 103.6 (2C, $C_{quart.}$); 103.3 (1C, CH_2); 62.0 (2C, CH_2); 41.5 (1C, CH_2); 39.4 (1C, CH_2); 37.2 (1C, CH_2); 15.0 ppm (2C, CH_3); IR (ATR): $\tilde{\nu}$ = 3270, 3091, 2984, 1719, 1661, 1451, 1298, 1268, 1177, 1091, 1022, 955, 723 cm^{-1}; HRMS: (ESI) *m/z* = 410.1310 [MH^+], calc.: 410.1325

7-Methoxy-7-oxoheptanoic acid (10c):[38] Compound **9** was synthesised according to the procedure of Cisneros *et al.* from pimelic acid (3.02 g, 18.84 mmol) and then refluxed in anhydrous methanol (10 mL) for 5 h. After removal of the solvent under reduced pressure the residue was purified by distillation (100°C, 1.2 · 10^{-2} mbar) to yield **10c** as a colorless oil (1.67 g, 51 % over 2 steps). ^{1}H-NMR (300 MHz, $CDCl_3$, 25°C): δ = 10.82 (s, 1H, OH); 3.63 (s, 3H, CH_3); 2.32 (t, ^3J =7.5 Hz, 2H, CH_2); 2.29 (t, ^3J =7.6 Hz, 2H, CH_2); 1.70-1.54 (m, 4H, CH_2); 1.41-125 ppm (m, 2H, CH_2); ^{13}C-NMR (75 MHz, $CDCl_3$, 25°C): δ = 179.8 (1C, C=O); 174.1 (1C, C=O); 51.4 (1C, CH_3); 33.7 (2C, CH_2); 28.4 (1C, CH_2); 24.4 (1C, CH_2); 24.2 ppm (1C, CH_2); IR (ATR): $\tilde{\nu}$ = 2950, 2866, 1733, 1708, 1437, 1198, 1171 cm^{-1}; HRMS: (EI) *m/z* = 175.0964 [MH^+], calc.: 175.0965.

Methyl 8,8,8-trifluoro-7-oxooctanoate (11c): Compound **11c** was synthesised similar to the procedure described by Biovin.[40] To a stirred solution of pimelic acid monomethyl ester **10c** (1.36 g, 7.81 mmol) in anhydrous DCM (20 mL) was added one drop of anhydrous DMF. After cooling to 0°C oxalyl chloride (1.2 mL, 15.62 mmol, 2.0 eq.) was added slowly and the solution was stirred for 18 h at RT. After removing of all volatile compounds under reduced pressure the corresponding acid chloride of **10c** was dissolved in anhydrous DCM (50 mL) and cooled to 0°C. Treated with trifluoroacetic anhydride (4.4 mL, 31.25 mmol, 4.0 eq.) and pyridine (3.8 mL, 46.87 mmol, 6.0 eq.) the solution was stirred for 30 min at 0°C. Ice water (20 mL) was added slowly and the solution was then stirred additionally for 60 min. After the addition of distilled water (100 mL) to the solution and the separation of the organic phase, the inorganic phase was extracted with DCM (4x50 mL). The combined organic phases were washed with a saturated aqueous solution of NaCl, dried over $MgSO_4$ and concentrated under reduced pressure. The residue was purified by silica gel chromatography (DCM/PE 1:1) to obtain **11c** as a pale yellow oil (1.58 g, 58 %), which was contaminated with small amounts of starting material which cannot separated from the product. ^{1}H-NMR (300 MHz, $CDCl_3$, 25°C): δ = 3.65 (s, 3H, CH_3); 2.71 (t, ^3J = 7.2 Hz, 2H, CH_2); 2.31 (t, ^3J = 7.4 Hz, 2H, CH_2); 1.75-1.53 (4H, CH_2); 1.43-1.28 ppm (m, 2H, CH_2); ^{13}C-NMR (75 MHz, $CDCl_3$, 25°C): δ = 191.4 (q, ^2J(C,F) = 34.8 Hz, 1C, C=O); 176.0 (1C, C=O); 115.5 (q, ^1J(C,F) = 292.0 Hz, 1C, CF_3); 52.3 (1C, CH_3); 36.0 (1C, CH_2); 33.7 (1C, CH_2); 28.0 (1C, CH_2); 24.4 (1C, CH_2); 21.9 ppm (1C, CH_2); ^{19}F-NMR (282 MHz, $CDCl_3$, 25°C): δ = -80.0 ppm (s, 3F, CF_3); IR (ATR): $\tilde{\nu}$ = 2952, 2869, 1763, 1735, 1438, 1404, 1368, 1291, 1203, 1152, 1023 cm^{-1}.

7,7,7-Trifluoro-6-oxoheptanoic acid (12b):[36] The carboxylic acid **12b** was synthesised similar to the procedure described by Frey *et al.*.[36] The trifluoromethyl ketone **11b** (1.02 g, 4.81 mmol) was dissolved in THF (20 mL) at RT and treated with an aqueous solution of LiOH (2 M, 24 mL) for 8 h. Then the reaction mixture was washed with MTBE (2x10 mL) and acidified with aqueous HCl (1 N) to pH 2. The inorganic phase was extracted with EtOAc (4x 20mL) and the combined organic phases were dried ($MgSO_4$), filtered and concentrated under reduced pressure. The desired trifluoromethyl ketone **12b** was obtained as a white solid (0.67 g, 70 %) and was used without further purification. The analytical data are in agreement with those reported.

8,8,8-Trifluoro-7-oxooctanoic acid (12c):[36] The trifluoromethyl ketone **12c** was synthesised from the methylester **11c** (737.5 mg, 3.26 mmol) by following the procedure described above for compound **12b.** The crude product was purified by silica gel chromatography (DCM/MeOH 30:1) to afford the trifluoromethyl ketone **12c** as highly viscous oil (425.1 mg, 61 %). The analytical data are in agreement with those reported.

***N*-(2-(2-(4,8-Dibutyrylbenzo[1,2-d:4,5-d']bis([1,3]dioxole)-2-yl)acetamido)ethyl)-6,6,6-trifluoro-5-oxohexanamide (13a):** To a mixture of the carboxylic acid **12a** (20.0 mg, 108.63 µmol, 1.5 eq.), DIEA (26.0 µL, 149.26 µmol, 2.0 eq.) and TBTU (35.0 mg, 109.00 µmol, 1.5 eq.) in anhydrous DMF (1.5 mL) was added the amine **6** (38.7 mg, 74.36 µmol, 1.0 eq.). After 16 h the solvent was removed under reduced pressure and the residue was dissolved in DCM and worked up with aqueous HCl (1 N) and saturated aqueous NaCl. The organic phase was dried ($MgSO_4$), filtered and concentrated under reduced pressure and the crude product was purified by silica gel chromatography (DCM/MeOH/TEA 100:1:0.1). After washing with saturated aqueous NaCl and drying over $MgSO_4$ the trifluoromethyl ketone **13a** was obtained as an orange solid (37.7 mg, 89 %). NMR spectra have shown that the title compound exists as a mixture of two tautomers. Which tautomer is predominant depends on the solvent. The present data shows a 1:1 mixture (judged by ^{1}H- und ^{19}F-NMR). R_f = 0.49 (DCM/MeOH 10:1); m. p.: 124-127°C; ^{1}H-NMR (300 MHz, $CDCl_3$, 27°C): δ = 6.90 (bt, 0.5H, NH); 6.74 (bt, 0.5H, NH); 6.68-6.49 (1.5H, NH, CH); 6.18-6.05 (2H, CH_2); 4.26-4.12 (m, 0.5H, CH); 3.87-3.73 (m, 0.5H, CH); 3.56 - 3.24 (3H, CH_2); 3.00 - 2.78 (6H, CH_2); 2.57-2.35 (1.5H, CH, CH_2); 2.29 (t, ^3J = 7.1 Hz, 1H, CH_2); 2.12-1.93 (1.5H, CH, CH_2); 1.91-1.62 (6H, CH_2); 0.97 ppm (t, ^3J = 7.4 Hz, 6H, CH_3); ^{13}C-NMR (75 MHz, $CDCl_3$, 27°C): δ = 196.7 (2C, C=O); 196.6 (2C, C=O); 172.7 (1C, C=O); 172.3 (1C, C=O); 168.2 (1C, C=O); 167.0 (1C, C=O); 141.2 (2C, $C_{quart.}$); 140.4 (2C, $C_{quart.}$); 110.6 (2C, $C_{quart.}$); 110.5 (2C, $C_{quart.}$); 110.1 (1C, CH); 102.6 (1C, CH_2); 102.5 (1C, CH_2); 45.7 (2C, CH_2); 42.2 (1C, CH_2); 39.9 (1C, CH_2); 39.8 (1C, CH_2); 35.5 (1C, CH_2); 34.2 (1C, CH_2); 31.6 (1C, CH_2); 18.2 (1C, CH_2); 17.1 (2C, CH_2); 17.0 (2C, CH_2); 13.7 ppm (2C, CH_3); ^{19}F-NMR (282 MHz, $CDCl_3$, 25°C): δ = -77.6 (s, 3F), -79.7 ppm (s, 3F); IR (ATR): $\tilde{\nu}$ = 3283, 2964, 2877, 1685, 1660, 1438, 1283, 1204, 1120, 1093 cm^{-1}; HRMS: (EI) *m/z* = 572.1986 [M^+], calc.: 572.1982.

Diethyl 2-(2-oxo-2-((2-(6,6,6-trifluoro-5-oxohexanamido)ethyl)amino)ethyl)benzo[1,2-d:4,5-d']bis([1,3]dioxole)-4,8-dicarboxylate (14a): Following the procedure described above for **13a**, the trifluoromethyl ketone **14a** was obtained from the carboxylic acid **12a** (18.0 mg, 97.77 µmol, 1.3 eq.), DIEA (26 µL, 149.26 µmol, 2.0 eq.), TBTU (33.59 mg, 104.61 µmol, 1.4 eq.) and the amine **7** (38.7 mg, 73.80 µmol) in anhydrous DMF (1.5 mL) as a yellow solid (35.7 mg, 84 %). NMR spectra have shown that the title compound exists as a mixture of two tautomers. Which tautomer is predominant depends on the solvent. The present data shows a 1:1 mixture (judged by ^{1}H- und ^{19}F-NMR). R_f = 0.47

(DCM/MeOH 10:1); m. p.: 155-158°C; ^{1}H-NMR (300 MHz, $CDCl_3$, 25°C): δ = 6.78 (bs, 0.5H, NH); 6.72-6.36 (2H, NH, CH); 6.11 (s, 2H, CH_2); 4.37 (q, ^3J = 7.1 Hz, 4H, CH_2); 4.25-4.11 (m, 0.5H, CH); 3.86-3.70 (m, 0.5H, CH); 3.61-3.20 (3H, CH_2); 3.02-2.88 (2H, CH_2); 2.82 (t, ^3J = 6.8 Hz, 1H, CH_2); 2.52-2.32 (1.5H, CH, CH_2); 2.27 (t, ^3J = 7.0 Hz, 1H, CH_2); 2.10-1.75 (m, 2.5H, CH_2); 1.38 ppm (t, ^3J= 7.1 Hz, 6H. CH_3); ^{13}C-NMR (75 MHz, $CDCl_3$, 25°C): δ = 172.6 (1C, C=O); 172.2 (1C, C=O); 168.3 (1C, C=O); 167.3 (1C, C=O); 161.9 (2C, C=O); 141.9 (2C, $C_{quart.}$); 141.2 (2C, $C_{quart.}$); 110.9 (1C, CH); 110.7 (1C, CH); 103.2 (2C, $C_{quart.}$); 102.9 (1C, CH_2); 61.7 (2C, CH_2); 42.2 (1C, CH_2); 41.7 (1C, CH_2); 40.3 (2C, CH_2); 39.6 (2C, CH_2); 35.5 (1C, CH_2); 34.1 (1C, CH_2); 32.3 (1C, CH_2); 31.5 (1C, CH_2); 18.1 (1C, CH_2); 15.4 (1C, CH_2); 14.2 ppm (2C, CH_3); ^{19}F-NMR (282 MHz, $CDCl_3$, 25°C): δ = -77.9 (s, 3F); -79.9 ppm (s, 3F); IR (ATR): $\bar{\nu}$ = 3405, 2976, 1720, 1654, 1449, 1296, 1176, 1078, 1023 cm^{-1}; HRMS: (EI) *m/z* = 576.1548 [M$^+$], calc.: 576.1567.

***N*-(2-(2-(4,8-Dibutyrylbenzo[1,2-d:4,5-d']bis([1,3]dioxole)-2-yl)acetamido)ethyl)-7,7,7-trifluoro-6-oxoheptanamide (13b):** Following the procedure described above for **13a**, the trifluoromethyl ketone **13b** was obtained from the carboxylic acid **12b** (20.0 mg, 108.63 µmol, 1.5 eq.), DIEA (26 µL, 149.26 µmol, 2.0 eq.), TBTU (35.0 mg, 109.00 µmol, 1.5 eq.) and the amine **6** (38.7 mg, 74.36 µmol) in anhydrous DMF (1.5 mL). Purifying by silica gel chromatography (DCM/MeOH/TEA 100:1:0.1) give the title compound as an orange solid (26.8 mg, 71 %). R_f = 0.47 (DCM/MeOH 10:1); m. p.: decomp. at 175°C; ^{1}H-NMR (300 MHz, $CDCl_3$, 25°C): δ = 6.82 (bs, 1H, NH); 6.65 (bs, 1H,-NH); 6.59 (t, ^3J = 4.8 Hz, 1H, CH); 6.11 (s, 2H, CH_2); 3.54-3.33 (4H, CH_2); 2.97-2.83 (6H, CH_2); 2.73 (bt, 2H, CH_2); 2.26 (bt, 2H, CH_2); 1.88-1.56 (8H, CH_2); 0.97 ppm (t, ^3J = 7.3 Hz, 6H, CH_3); ^{13}C-NMR (75 MHz, $CDCl_3$, 25°C): δ = 196.7 (2C, C=O); 173.3 (1C, C=O); 167.2 (1C, C=O); 141.2 (2C, $C_{quart.}$); 140.4 (2C, $C_{quart.}$); 110.6 (2C, $C_{quart.}$); 110.0 (1C, CH); 102.6 (1C, CH_2); 45.7 (2C, CH_2); 42.2 (1C, CH_2); 40.0 (1C, CH_2); 39.9 (1C, CH_2); 36.1 (1C, CH_2); 35.7 (1C, CH_2); 24.5 (1C, CH_2); 21.8 (1C, CH_2); 17.1 (2C, CH_2); 13.7 ppm (2C, CH_3); ^{19}F-NMR (282 MHz, $CDCl_3$, 25°C): δ = -79.8 ppm (s, 3F); IR (ATR): $\bar{\nu}$ = 3284, 2962, 2936, 2877, 1678, 1642, 1560, 1436, 1281, 1089 cm^{-1}; HRMS: (EI) *m/z* = 586.2128 [M$^+$], calc.: 586.2138.

Diethyl 2-(2-oxo-2-((2-(7,7,7-trifluoro-6-oxoheptanamido)ethyl)amino)ethyl)benzo[1,2-d:4,5-d']bis([1,3]dioxole)-4,8-dicarboxylate (14b): Following the procedure described above for **13a**, the trifluoromethyl ketone **14b** was obtained from the carboxylic acid **12b** (15.5 mg, 78.23 µmol, 1.1 eq.), DIEA (30 µL, 172.23 µmol, 2.5 eq.), TBTU (25.5 mg, 79.42 µmol, 1.1 eq.) and the amine **7** (36.6 mg, 69.79 µmol, 1.0 eq.) in anhydrous DMF (3.0 mL). Purifying by silica gel chromatography (DCM/MeOH/TEA 10:1:0.0→10:1:0.1) give the title compound as a yellow solid (36.5 mg, 89 %). R_f = 0.45 (DCM/MeOH 10:1); m. p.: decomp. at 182°C; ^{1}H-NMR (300 MHz, $CDCl_3$, 25°C): δ = 6.72 (bs, 1H, NH); 6.67-6.46 (2H, NH, CH); 6.11 (s, 2H, CH_2); 4.38 (q, ^3J = 7.1 Hz, 4H, CH_2); 3.57-3.30 (4H, CH_2); 3.02-2.83 (m, 2H, CH_2); 2.82-2.65 (m, 2H, CH_2); 2.36-2.12 (m, 2H, CH_2); 1.77-1.58 (m, 4H, CH_2); 1.37 ppm (t, ^3J = 7.2 Hz, 6H, CH_3); ^{13}C-NMR (126 MHz, $CDCl_3$, 25°C): δ = 161.9 (2C, C=O); 141.9 (2C, $C_{quart.}$); 141.2 (2C, $C_{quart.}$); 110.8 (1C, CH); 103.2 (2C, $C_{quart.}$); 102.9 (1C, CH_2); 61.7 (2C, CH_2); 42.2 (1C, CH_2); 40.0 (1C, CH_2); 39.9 (1C, CH_2); 36.1 (1C, CH_2); 35.7 (1C, CH_2); 24.5 (1C, CH_2); 21.8 (1C, CH_2); 14.2 ppm (2C, CH_3); ^{19}F-NMR (282 MHz, $CDCl_3$, 25°C): δ = -79.8 ppm (s, 3F); IR (ATR): $\bar{\nu}$ = 3276, 2943, 1710, 1659, 1557, 1451, 1294, 1262, 1156, 1080, 1025 cm^{-1}; HRMS: (EI) *m/z* = 590.1739 [M$^+$], calc.: 590.1723.

***N*-(2-(2-(4,8-Dibutyrylbenzo[1,2-d:4,5-d']bis([1,3]dioxole)-2-yl)acetamido)ethyl)-8,8,8-trifluoro-7-oxooctanamide (13c):** Following the procedure described above for **13a**, the trifluoromethyl ketone **13c** was obtained from the carboxylic acid **12c** (18.2 mg, 85.78 µmol, 1.1 eq.), DIEA (35 µL, 200.93 µmol, 2.7 eq.), TBTU (27.3 mg, 85.02 µmol, 1.1 eq.) and the amine **6** (39.2 mg, 75.32 µmol, 1.0 eq.) in anhydrous DMF (4.0 mL). Purifying by silica gel chromatography (DCM/MeOH/TEA 10:1:0.0→10:1:0.1) give the title compound as an orange solid (40.3 mg, 90 %). R_f = 0.53 (DCM/MeOH 10:1); m. p.: 185-186°C; ^{1}H-NMR (300 MHz, $CDCl_3$, 25°C): δ = 6.72 (bt, 1H, NH); 6.60 (bt, 1H, NH); 6.59 (t, ^3J = 5.3 Hz, 1H, CH); 6.11 (s, 2H, CH_2); 3.47-3.36 (4H, CH_2); 2.93-2.86 (6H, CH_2); 2.71 (t, ^3J = 7.1 Hz, 2H, CH_2); 2.22 (t, ^3J = 7.4 Hz, 2H, CH_2); 1.77-1.58 (8H, CH_2); 1.41-1.24 (m, 2H, CH_2); 0.97 ppm (t, ^3J = 7.4 Hz, 6H, CH_3); ^{13}C-NMR (75 MHz, $CDCl_3$, 25°C): δ = 196.6 (2C, C=O); 173.8 (1C, C=O); 167.0 (1C, C=O); 141.2 (2C, $C_{quart.}$); 140.4 (2C, $C_{quart.}$); 110.6 (1C, CH); 110.1 (2C, $C_{quart.}$); 102.6 (1C, CH_2); 45.7 (2C, CH_2); 42.2 (1C, CH_2); 40.2 (1C, CH_2); 39.9 (1C, CH_2); 36.1 (1C, CH_2); 35.9 (1C, CH_2); 28.2 (1C, CH_2); 25.0 (1C, CH_2); 22.0 (1C, CH_2); 17.1 (2C, CH_2); 13.7 (2C, CH_3); ^{19}F-NMR (282 MHz, $CDCl_3$, 25°C): δ = -79.8 ppm (s, 3F); IR (ATR): $\bar{\nu}$ = 3275, 2933, 1710, 1658, 1557, 1451, 1293, 1262, 1155, 1079, 1051 cm^{-1}; HRMS: (EI) *m/z* = 600.2304 [M$^+$], calc.: 600.2295.

Diethyl 2-(2-oxo-2-((2-(8,8,8-trifluoro-7-oxooctanamido)ethyl)amino)ethyl)benzo[1,2-d:4,5-d']bis([1,3]dioxole)-4,8-dicarboxylate (14c): Following the procedure described above for **13a**, the trifluoromethyl ketone **14c** was obtained from the carboxylic acid **12c** (17.9 mg, 84.37 µmol, 1.1 eq.), DIEA (35 µL, 200.93 µmol, 2.7 eq.), TBTU (27.2 mg, 84.71 µmol, 1.1 eq.) and the amine **7** (39.2 mg, 74.75 µmol, 1.0 eq.) in anhydrous DMF (4.0 mL). Purifying by silica gel chromatography (DCM/MeOH/TEA 20:1:0.1) give the title compound as a yellow solid (44.4 mg, 98 %). R_f = 0.48 (DCM/MeOH 10:1); m. p.: decomp. at 195°C; ^{1}H-NMR (300 MHz, $CDCl_3$, 25°C): δ = 6.75 (bt, 1H, NH); 6.64-6.56 (1H, NH); 6.60 (t, ^3J = 5.3 Hz, 1H, CH); 6.11 (d, AB, *J* =1.6 Hz, 2H, CH_2); 4.38 (q, ^3J = 7.1 Hz, 4H, CH_2); 3.49-3.34 (4H, CH_2); 2.91 (d, ^3J = 5.3 Hz, 2H, CH_2); 2.71 (t, ^3J = 7.0 Hz, 2H, CH_2); 2.23 (t, ^3J = 7.4 Hz, 2H, CH_2); 1.73-1.58 (m, 4H, CH_2); 1.41-1.28 (m, 2H, CH_2); 1.37 ppm (t, ^3J = 7.1 Hz, 6H, CH_3); ^{13}C-NMR (75 MHz, $CDCl_3$, 25°C): δ = 167.3 (1C, C=O); 161.8 (2C, C=O); 141.9 (2C, $C_{quart.}$); 141.2 (2C, $C_{quart.}$); 110.8 (1C, CH); 103.2 (2C, $C_{quart.}$); 102.9 (1C, CH_2); 61.7 (2C, CH_2); 42.1 (1C, CH_2); 40.1 (1C, CH_2); 39.8 (1C, CH_2); 36.1 (1C, CH_2); 35.6 (1C, CH_2); 28.2 (1C, CH_2); 25.1 (1C, CH_2); 22.0 (1C, CH_2); 14.2 ppm (2C, CH_3); ^{19}F-NMR (282 MHz, $CDCl_3$, 25°C): δ = -79.5 ppm (s, 3F); IR (ATR): $\bar{\nu}$ = 3278, 2931, 1710, 1657, 1557, 1450, 1293, 1261, 1155, 1079, 1051 cm^{-1}; HRMS: (EI) *m/z* = 604.1869 [M$^+$], calc.: 604.1880.

Protein expression and purification of HDACs

The genes encoding the catalytical domains of HDAC4 (amino acids 648-1057), HDAC5 (amino acids 655-1122), HDAC7 (amino acids 518-952) and full length HDAC8 were codon optimised and ordered from GenScribt. The genes were delivered in a pUC57 plasmid and cloned into a pET14b-SUMO (HDAC8) or a pET14b-SUMO-CPD (HDAC4, 5 and 7) vector. All proteins were recombinantly expressed in *E.coli* BL21(DE3) as fusion proteins, whereby they were N-terminally fused to a 6xHis-SUMO tag.[43] HDACs 4, 5 and 7 were additionally fused to a C-terminal cysteine protease domain (CPD), which possess an autocatalytic activity and cuts itself from the HDAC upon induction by phytic acid.[44] Bacterial cultures were grown at 37 °C in LB media to an optical density at 600 nm of 0.6 - 0.8. The protein expression was induced by addition of 1 mM isopropyl-β-D-thiogalactopyranoside and the cells were further cultured overnight at 25 °C. Cells were harvested by centrifugation (15 min, 15.000x*g*, 4 °C) and the pellet was resuspended in lysis buffer (50 mM HEPES, pH 8.0, 300 mM NaCl). Cells were lysed by sonication and cell fragments were removed by centrifugation (30 min, 25000x*g*, 4 °C). The supernatant was loaded onto an immobilised metal affinity chromatography using a cOmplete His-Tag purification resin (Roche) which was equilibrated with lysis buffer. The resin was washed with 20 volumes of lysis buffer. For the CPD fusion constructs the resin

was afterwards incubated for one hour with 200 µM phytic acid in lysis buffer. The SUMO fusion proteins were eluted by addition of 100 mM imidazole in lysis buffer. The SUMO tag was cleaved by incubation with 20 µg Ulp 1 at 4 °C over night. The proteins were purified further by gelfiltration using a Sephadex 200 16/60 column equilibrated with HDAC buffer (50 mM HEPES, pH 8.0, 20 mM NaCl, 10 mM KCl). HDAC containing fractions were pooled and concentrated. The protein concentration was determined by using the bicinchoninic acid assay. Protein solutions were supplemented with 10% glycerol, flash frozen with liquid nitrogen and stored at -20 °C.

Enzyme activity assay

The HDAC activity assay was conducted as described elsewhere.[26] In brief a serial dilution of the DBD probe or inhibitor in assay buffer (25 mM Tris-HCl, pH 8.0, 75 mM KCl, 0.001% Pluronic F-127) was placed in a black 96-well microtiter plate (Greiner) and incubated with 1 nM of the respective HDAC isoform for 30 min at 30 °C. The reaction was then initiated by addition of either 50 µM Boc-Lys(Ac)-AMC (for HDAC1, 2, 3 and 6) or 20 µM Boc-Lys(trifluoracetyl)-AMC (for HDAC4, 5, 7 and 8) as substrate. After an incubation for 60 minutes at 30 °C the reaction was stopped by addition of 20 µM SAHA or SATFMK and the deacetylated substrate was converted into a fluorescent product by addition of 0.5 mg/ml trypsin. The release of AMC was followed in a micro plate reader and correlated to enzyme activity. Dose-response curves were generated using graph pad prism and fitted to the following four parameter logistic model yielding the respective IC_{50}-value[45]

$$EA = E_0 + \frac{(E_{max} - E_0)}{1+10^{[(\log IC_{50} - x)h]}} \quad (1)$$

where *EA* denotes enzyme activity at a certain inhibitor concentration *x* and E_{max} and E_0 are the determined enzyme activity at no and complete inhibition; IC_{50} denotes the inhibitor concentration, at which half of the enzyme is inhibited and *h* is the hill slope.

Isothermal titration calorimetry

For the validation of the K_I-values determined by the fluorescence life time binding assay binding of SATFMK and PDF306 to HDAC4 and HDAC8 was investigated by ITC. Therefore, 20 to 40 µM HDAC in HDAC buffer was placed in the sample cell of a PEAQ-ITC instrument (Malvern Instruments Ltd) 25 °C. The syringe was loaded with 100 to 200 µM of the inhibitor suspended in HDAC buffer. To minimise the heat of dilution the DMSO and glycerol concentrations were adjusted to be identical in the sample cell and syringe. Nevertheless, the resulting final DMSO concentrations of up to 2% resulted in a reduction of the binding active HDAC concentration which resulted in a observed stoichiometry between 0.13 and 0.4. The measurements were carried out at 25 °C and the inhibitor was titrated by injecting 19 times 2 µl into the sample cell with a spacing of 150 to 300 s. The amount of released heat for each injection was determined by integrating the area under the curve by using the MicroCal PEAQ-ITC Analysis software. The resulting data points were the fitted to a one site binding model supplied with the software.

Fluorescence life time binding assay

In order to determine the equilibrium dissociation constant of the binding of the acyl DBD ligands **13a-c** to HDAC4, 5, 7 and 8 a serial dilution of the respective HDAC was placed in the afore mentioned microtiter plate and mixed with 25 to 125 nM of the DBD ligand. After incubation for 30 minutes at 25 °C the fluorescence decay was measured using a LF502 nanoscan instrument from Berthold Detection Systems GmbH (Pforzheim, Germany) behind a 630 nm band-pass filter after pulse excitation at 456 nm. For the binding of the ester DBD ligands **14a-c** the experiments were conducted under the same conditions, but the band-pass filter was exchanged to 520 nm and the pulse excitation occurred at 405 nm. Binding of the DBD ligands resulted in an increased FLT, which was exploited to determine the binding degree (B.D.) according to

$$B.D. = \frac{A - A_{min}}{A_{max} - A_{min}} \quad (2)$$

where A denotes the FLT in the presence of a certain enzyme concentration of interest, A_{min} the FLT in the absence of enzyme and A_{max} the FLT in the presence of saturating enzyme concentrations.

From the determined binding isotherms the equilibrium dissociation constant, K_d, can be fitted by exploiting the following equation

$$B.D. = \frac{[EL]}{[L]_0} = \frac{1}{2[L]_0}\left([E]_0 + [L]_0 + K_d - \sqrt{([E]_0 + [L]_0 + K_d)^2 - 4[L]_0[E]_0}\right) \quad (3)$$

where [*EL*] is the equilibrium concentration of the complex between the enzyme, *E*, and the respective DBD-ligand, *L*. Initial concentrations are marked by the subscript 0 and other concentrations refer to the chemical equilibrium state.

For the determination of the inhibitor binding constant K_I of unlabeled HDAC inhibitors a serial dilution of the respective inhibitor in assay buffer supplemented with 0.125 µM of the respective DBD probe was placed in the afore mentioned microtiter plate. 0.45 to 0.8 µM of HDAC8 or HDAC4 were added and the plates were incubated for 1 hour at room temperature. Afterwards the FLT of the DBD probe was determined as stated above. The binding reaction was analyzed with a simple competition model (E+L= EL and E+I=EI) where the inhibitor, I, binds to the enzyme, E, and forms the enzyme-inhibitor complex, EI, which is in competition to the formation of the complex EL between the DBD probe, L, and the enzyme

$$B.D. = \frac{1}{2[E]_0}\left(-\frac{K_I + \frac{K_d}{[L]_0}(K_I + [I]_0 - [E]_0)}{\frac{K_d}{[L]_0}\left(\frac{K_d}{[L]_0}+1\right)}\right) + \sqrt{\left(\frac{K_I + \frac{K_d}{[L]_0}(K_I + [I]_0 - [E]_0)}{\frac{K_d}{[L]_0}\left(\frac{K_d}{[L]_0}+1\right)}\right)^2 + \frac{4[E]_0 K_I [L]_0}{K_d\left(\frac{K_d}{[L]_0}+1\right)}} \quad (4)$$

Acknowledgements

The work has been supported by the Deutsche Forschungsgemeinschaft (DFG Grant ME 3122/2-1).

Keywords: Fluorescent probes • Hydrolases • High-throughput screening

[1] I. Hoshino, H. Matsubara, *Surg. Today.* **2010**, *40*, 809–15.

[2] D.-M. Chuang, Y. Leng, Z. Marinova, H.-J. Kim, C.-T. Chiu, *Trends Neurosci.* **2009**, *32*, 591–601.

[3] K. T. Andrews, A. Haque, M. K. Jones, *Immunol. Cell Biol.* **2011**, *90*, 66–77.

[4] X.-J. Yang, E. Seto, *Nat. Rev. Mol. Cell Biol.* **2008**, *9*, 206–18.

[5] I. Gregoretti, Y.-M. Lee, H. V. Goodson, *J. Mol. Biol.* **2004**, *338*,17–31.

[6] S. Yoon, G. H. Eom, *Chonnam Med. J.* **2016**, *52*,1–11.

[7] P. A. Marks, R. Breslow, Nat. Biotechnol. **2007**, *25*, 84–90.

[8] P. A. Marks, W.-S. Xu, *J. Cell. Biochem.* **2009**,*107*, 600–608.

[9] A. Lahm, C. Paolini, M. Pallaoro, M. Nardi, P. Jones, P. Neddermann, S. Sambucini, M. J. Bottomley, P. lo Surdo, A. Carfí, U. Koch, R. de Francesco, C. Steinkühler, P. Gallinari, *Proc. Natl. Acad. Sci. U. S. A.* **2007**, *104*,17335–17340.

[10] A. Clocchiatti, E. di Giorgio, F. Demarchi, C. Brancolini, *Cell. Signalling* **2013**, *25*, 269–276.

[11] M. Lobera, K. P. Madauss, D. T. Pohlhaus, G. Q. Wright, M. Trocha, D. R. Schmidt, E. Baloglu, R. P. Trump, M. S. Head, G. A. Hofmann, M. Murray-Thompson, B. Schwartz, S. Chakravorty, Z. Wu, P. K. Mander, L. Kruidenier, R. A. Reid, W. Burkhart, B. J. Turunen, J. X. Rong, C. Wagner, M. B. Moyer, C. Wells, X. Hong, J. T. Moore, J. D. Williams, D. Soler, S. Gosh, M. A. Nolan, *Nat. Chem. Biol.* **2013**, *9*, 319–325

[12] P. Jones, S. Altamura, R. de Francesco, P. Gallinari, A. Lahm, P. Neddermann, M. Rowley, S. Serafini, C. Steinkühler, *Bioorg. Med. Chem. Lett.* **2008**, *18*, 1814–1819

[13] W. Fischle, F. Dequiedt, M. J. Hendzel, M. G. Guenther, M. A. Lazar, W. Voelter, E. Verdin, *Mol. Cell.* **2002**, *9*, 45-57

[14] A: Clocchiatti, E. di Giorgio, S. Ingrao, F.-J. Meyer-Almes, C. Tripodo, C. Brancolini, *FASEB J.* **2013**, *27*, 942–954.

[15] E. di Giorgio, A. Clocchiatti, S. Piccinin, A. Sgorbissa, G. Viviani, P. Peruzzo, S. Romeo, S. Rossi, A. P. dei Tos, R. Maestro, C. Brancolini, *Mol. Cell. Biol.* **2013**, *33*, 4473–4491

[16] D. B. Sparrow, E. A. Miska, E. Langley, S. Reynaud-Deonauth, S. Kotecha, N. Towers, G. Spohr, T. Kouzarides, T. J. Mahun, *EMBO J.* **1999**, *18*, 5085–5098

[17] C. H, Arrowsmith, C. Bounta, P. V. Fish, K. Lee, M. Schapira, *Nat. Rev. Drug Discov.* **2012**,*11*, 384–400

[18] J. E. Bradner, N. West, M. L. Grachan, E. F. Greenberg, S. J. Haggarty, T. Warnow, R. Mazitschek, *Nat. Chem. Biol.* **2010**, *6*, 238–243

[19] S. Mujtaba, L. Zeng, M. M. Zhou, *Oncogene* **2007**, *26*, 5521–5527

[20] E. di Giorgio, E. Gagliostro, C. Brancolini, *Cell. Mol. Life Sci.* **2015**, *72*, 73–86

[21] H. L. Fitzsimons, *Neurobiol. Learn Mem.* **2015**, *123*, 149–158

[22] M. Mielcarek, D. Zielonka, A. Carnemolla,J. T. Marcinkowski, F. Guidez, *Front. Cell. Neurosci.* **2015**, *9*, 42.

[23] C. A. Luckhurst, P. Breccia, A. J. Stott, O. Aziz, H. L. Birch, R. Bürli, S. J. Hughes, R. E. Jarvis, M. Lamers, P. M. Leonard, K. L. Matthews, G. McAllister, S. Pollack, E. Saville-Stones, G. Wishart, D. Yates, C. Dominguez, *ACS Med. Chem. Lett.* **2015**, *7*, 34–39.

[24] M.-C. Choi, T. J. Cohen, T. Barrientos, B. Wang, M. Li, B. J. Simmons, J. S. Yang, G. A. Cox, Y. Zhao, T. P. Yao, *Mol. Cell.* **2012**, *47*, 122–132.

[25] N. A. Wolfson, C. A. Pitcairn, E. D. Sullivan, C. G. Joseph, C. A. Fierke, *Anal. Biochem.* **2014**, *456*, 61–69

[26] D. Wegener, C. Hildmann, D. Riester, A. Schwienhorst, *Anal. Biochem.* **2003**, *321*, 202–208.

[27] F. Halley, J. Reinshagen, B. Ellinger, M. Wolf, A. L. Niles, N. J. Evans, T. A. Kirkland, J. M. Wagner, M. Jung, P. Gribbon, S. Gul, *J. Biomol. Screening* **2011**,*16*,1227–1235.

[28] D. Riester, D. Wegener, C. Hildmann, A. Schwienhorst, *Biochem. Biophys. Res. Commun.* **2004**, *324*, 1116–1123.

[29] R. K. Singh, T. Mandal, N. Balasubramanian, G. Cook, D. Srivastava, *Anal. Biochem.* **2011**, *408*, 309–315.

[30] D, Riester, C. Hildmann, P- Haus, A. Galetovic, A. Schober, A. Schwienhorst, F.-J. Meyer-Almes, *Bioorg. Med. Chem. Lett.* **2009**,*19*, 3651–3656.

[31] C. Meyners, M. G. Baud, M. J. Fuchter, F.-J. Meyer-Almes, *J. Mol. Recognit.* **2014**, *27*, 160–72.

[32] L. Neumann, K. von König, D. Ullmann, *Methods Enzymol.* **2011**, *493*, 299–320.

[33] C. Meyners, R. Wawrzinek, A. Krämer, S. Hinz, P. Wessig, F.-J. Meyer-Almes, *Anal. Bioanal. Chem.* **2014**, *406*,4889–4897.

[34] C. Micelli, G. Rastelli, *Drug Discovery Today* **2015**, *20*, 718–735

[35] A. S. Madsen, H. M. Kristensen, G. Lanz, C. A. Olsen, *ChemMedChem* **2014**, *9*, 614–626.

[36] R. R. Frey, C. K. Wada, R. B. Garland, M. L. Curtin, M. R. Michaelides, J. Li, L. J. Pease, K. B. Glaser, P. A. Marcotte, J. J. Bouska, S. S. Murphy, S. K. Davidsen, *Bioorg. Med. Chem. Lett.* **2002**, *12*, 3443–3447.

[37] R. Wawrzinek, J. Ziomkowska, J. Heuveling, M. Mertens, A. Herrmann, E. Schneider, P. Wessig, *Chem. – Eur. J.* **2013**,*19*, 17349–17357.

[38] J. A. Cisneros, E. Björklund, I. González-Gil, Y. Hu, A. Canales, F. J. Medrano, A. Romero, S. Ortega-Gutiérrez, C. J. Fowler, M. L. López-Rodríguez, *J. Med. Chem.* **2012**, 55, 824–836.

[39] T. Okano, T. Sakaida, S. Eguchi, *J. Org. Chem.* **1996**, *61*, 8826–8830.

[40] J. Boivin, L. el Kaim, S. Z. Zard, *Tetrahedron* **1995**, *51*, 2573–2584.

[41] T. K. Nielsen, C. Hildmann, D. Riester, D. Wegener, A: Schwienhorst, R. Ficner, *Acta Crystallogr., Sect. F: Struct. Biol. Cryst. Commun.* **2007**, *63*, 270–273.

[42] P. Jones, M. J. Bottomley, A. Carfí, O. Cecchetti, F. Ferrigno, P. L. Surdo, J. M. Ontoria, M. Rowley, R. Scarpelli, C. Schultz-Fademrecht, C. Steinkühler, *Bioorg. Med. Chem. Lett.* **2008**, *18*, 3456–3461.

[43] M. P. Malakhov, M. R. Mattern, O. A. Malakhova, M. Drinker, S. D. Weeks, T. R. Butt, *J. Struct. Funct. Genomics* **2004**, *5*, 75–86.

[44] A. Shen, P. J. Lupardus, M. Morell, E. L. Ponder, A. M. Sadaghiani, K. C. Garcia, M. Bogyo, *PloS one*, **2009**, *4*, e8119.

[45] A. Vølund, *Biometrics* **1978**, *34*, 357–365.

10.1002/chem.201605140

WILEY-VCH

Entry for the Table of Contents (Please choose one layout)

Layout 1:

FULL PAPER

Text for Table of Contents

((Insert TOC Graphic here: max. width: 5.5 cm; max. height: 5.0 cm))

*Author(s), Corresponding Author(s)**

Page No. – Page No.

Title

Layout 2:

FULL PAPER

((Insert TOC Graphic here; max. width: 11.5 cm; max. height: 2.5 cm))

*Author(s), Corresponding Author(s)**

Page No. – Page No.

Title

Text for Table of Contents